



Synthesis and Tuning the Structural, Optical and Electrical Behavior of PVA-SiC-BaTiO₃ Polymer Nanostructures for Photonics and Electronics Nanodevices

Majeed Ali Habeeb¹ · Waleed Khalid Kadhim¹

Received: 31 August 2023 / Accepted: 5 October 2023 / Published online: 30 October 2023

© The Author(s), under exclusive licence to Springer Science+Business Media, LLC, part of Springer Nature 2023

Abstract

This study aims to fabricate thick films of polyvinyl alcohol containing (SiC-BaTiO₃) nanoparticles in order to improve their structural, optical, and electrical characteristics. The (PVA-SiC-BaTiO₃) nanocomposite films are made utilize the casting method. According to optical microscope images, the (SiC-BaTiO₃) nanoparticles create a persistent network inside the polymer compared to pure (PVA). FTIR reveals that the peak position, peak shape, and intensity are shifting. When (SiC-BaTiO₃) nanoparticle concentrations were increased to (6 wt%), optical tests revealed that the absorbance of (PVA-SiC-BaTiO₃) nanocomposites enhanced from 50 to 98%. Meanwhile, the energy gap of (PVA-SiC-BaTiO₃) nanocomposites declined from (4.42 to 3.56) eV and from (4.1 to 2.85) eV for the allowed and forbidden indirect transitions, respectively. These findings could be important for using (PVA-SiC-BaTiO₃) nanostructures in diverse optics applications and nanotechnology. As well as an increase in optical parameters including optical conductivity, real and imaginary dielectric constants, refractive index, absorption coefficient, and extinction coefficient. The dielectric loss (ϵ'') and dielectric constant (ϵ') for nanocomposites reduce as the frequency of the applied electrical field rises but increase as the concentration of nanoparticles (NPs) rises. When the (SiC-BaTiO₃) concentration reached (6 wt%) at a frequency of 100 Hz, A.C. electrical conductivity ($\sigma_{a.c}$) and dielectric constant increases by around 90% and 130%, respectively. Based on the results, doping PVA with (SiC-BaTiO₃) NPs enhanced the optical, structural, and A.C electrical properties, making the (PVA-SiC-BaTiO₃) nanostructures promising materials for various optoelectronic nanodevices.

Keywords PVA · SiC-BaTiO₃ nanoparticles · Nanocomposites · Optical and electrical properties · Nanodevices

1 Introduction

Polymeric nanocomposites are utilized in a broad range of applications like sensors, integrated circuits, devices for optoelectronics, photovoltaic cells, and reflecting materials [1, 2]. The electro-optical and structural properties of polymers were modified using nanomaterials to produce a superimposed effect, according to the purpose of the study and in any field of application [3]. The advantages of using these polymeric materials in electrical applications and

their excellent stability make them ideal for optoelectronic applications, the possibility of fabricating devices for optical uses, and improving electrical properties. Utilizing fillers or resizing these components in the matrix of polymers, their physical properties can be enhanced [4, 5]. Modifications that alter the optical characteristics of polymer nanocomposites and the production of novel nanocomposites present a major obstacle to researchers looking for materials with distinct properties. Many nanomaterials, such as metal oxides, iron, copper, and graphene oxide, can be used as fillers in polymer matrices, and to discover optical parameters for industrial applications, they must modify their optical properties and produce nanocomposites that meet the demand for electronic applications accelerating in global markets [6, 7]. The intent is to produce transparent films with excellent electrical and optical attributes and appropriate dielectric force, and polyvinyl alcohol (PVA) can serve as a suitable host material for a variety of nanoparticles [8, 9].

✉ Majeed Ali Habeeb
pure.majeed.ali@uobabylon.edu.iq

Waleed Khalid Kadhim
welidkhalid37@gmail.com

¹ College of Education for Pure Sciences, Department of Physics, University of Babylon, Babil, Iraq

Barium titanate (BaTiO_3) is a ceramic ferroelectric substance with a large dielectric constant and low dielectric loss. This gives it an advantage in the manufacture of various types of electrical circuits and capacitors. The properties of polymeric films filled with ceramics are of wide interest, such as their excellent flexibility, high dielectricity, and thermal fastness [10, 11]. Previous studies using different concentrations of (BaTiO_3) indicated its effect on the underlying structural makeup and electrical traits of (PVA) matrix, as well as an improvement in properties with increasing filler concentration [12]. Another study found that adding part of (BaTiO_3) to another polymer increased the dielectric constant, improved mechanical properties, and increased dielectric loss [13, 14]. A semiconductor made of silicon and carbon is known as silicon carbide (SiC) nanoparticles. It is utilized in a variety of applications, including those that demand a load capacity, like those in the automobile sector, and electrical ones that require high voltages, such as those for light-emitting diodes (LEDs) [15, 16]. The study of silicon carbide (SiC) has never ended since, as a ceramic, it inherits the amazing qualities of ceramic building materials, such as resistance to corrosion, high strength, and elevated hardness. SiC may be utilized as a raw material for advanced refractories, functional materials, and ceramics because of its outstanding high-temperature uniqueness, including oxidation resistance, low thermal expansion coefficient, and elevated thermal conductivity. SiC has increasingly gained significance due to its broadband gap with the expansion of electronic goods manufacturing in recent years. Among the most promising materials for fourth-generation semiconductors, (SiC) is attractive for use in large-frequency semiconductor devices [17, 18]. In this work, silicon carbide (SiC) and barium titanate (BaTiO_3) nanoparticles were used to improve the structural, optical, and electrical properties of (PVA-SiC- BaTiO_3) nanocomposites for employed in different optoelectronic nanodevices.

2 Experimental and Methods

Films of nanocomposites were created from (PVA), silicon carbide nanoparticles (SiC) and barium titanate (BaTiO_3), using the casting manner. Pure (PVA) was placed in 35 ml of distilled water, to get a more homogenous solution by swirling with a magnetic stirrer at 70 °C for 40 min. Barium titanate (BaTiO_3) and silicon carbide (SiC) nanoparticles were added to the polymer at (2, 4, and 6) wt%, respectively, after the solution was dried at room temperature for four days, polymer nanocomposites were produced. The PVA-SiC- BaTiO_3 nanocomposites were extracted from

the petri dish and used for measurement. By using an optical microscope (OM) from Olympus (model Nikon, Top View/73,346) with a (10X) magnifying lens and a camera for microscopy, the structural properties of nanocomposites were investigated. Fourier transfer infrared spectroscopy is used to assess (NCs) made of (PVA-SiC- BaTiO_3) samples in the range of wave numbers of 500–4000 cm^{-1} . Using a Shimadzu -UV-1800- spectrophotometer, the optical features of (PVA-SiC- BaTiO_3) NCs in the wavelength range (200–800 nm) were evaluated.

The equation presented as follows is used to compute absorbance [19]:

$$A = \frac{I_a}{I_0} \quad (1)$$

Where I_0 denotes the intensity of incident light, I_a denotes the intensity of light that is absorbed by the medium. Transmittance (T) may be calculated using the following equation [20]:

$$T = 10^{-A} \quad (2)$$

All films' absorbance coefficients(α) were calculated using the following equation [20]:

$$\alpha = \frac{2.303A}{t} \quad (3)$$

Where(t)thicknessofsample. Optical energy gap computed from formula [21]:

$$B(h\nu - E_g^{Opt.})^r = \alpha h\nu \quad (4)$$

Where B is a constant, (h ν)indicates the photon energy, and ($E_g^{Opt.}$) is the optical energy gap when r = 3" the forbidden indirect transition " and r = 2(the indirect transition of allowed). The extinction coefficient (k) was obtained using the equation shown below [22]:

$$k = \frac{\alpha \lambda}{4\pi} \quad (5)$$

Where the absorption coefficient is (α)and the wavelength is (λ). Computed refractive index(n)from equation [23]:

$$n = \sqrt{4R - \frac{k^2}{(R-1)^2} - \frac{(R+1)}{(R-1)}} \quad (6)$$

Where (R) reflection. There are two sections to the dielectric constant:- the (real and imaginary) parts (ϵ_1 , ϵ_2). Each of the real and imaginary parts may be determined using the formulae below [24]:

$$\epsilon_1 = n^2 - k^2 \quad (7)$$

$$\epsilon_2 = 2nk \quad (8)$$

The optical conductivity(σ) is calculated using the following formula [25]:

$$\sigma = \frac{\alpha nc}{4\pi} \quad (9)$$

Between 10^2 Hz and 5×10^6 Hz, using an (LCR meter-HIOKI-3532-50 HI-TESTER), the dielectric properties of nanocomposites were evaluated. The formula for determining the dielectric constant (ϵ') is as follows [26]:

$$\epsilon' = \frac{C_p}{C_0} \quad (10)$$

Capacity is indicated by (C_p), while a vacuum capacitor is indicated by (C_0). Dielectric loss (ϵ'') is computed using the equation [27]:

$$\epsilon'' = \epsilon' D \quad (11)$$

(D) is expresses displacement. The A.Celectrical conductivity is determined ,as shown below [28]:

$$\sigma_{a.c} = \omega \epsilon'' \epsilon_0 \quad (12)$$

Where (ω): angular frequency.

3 Results and Discussions

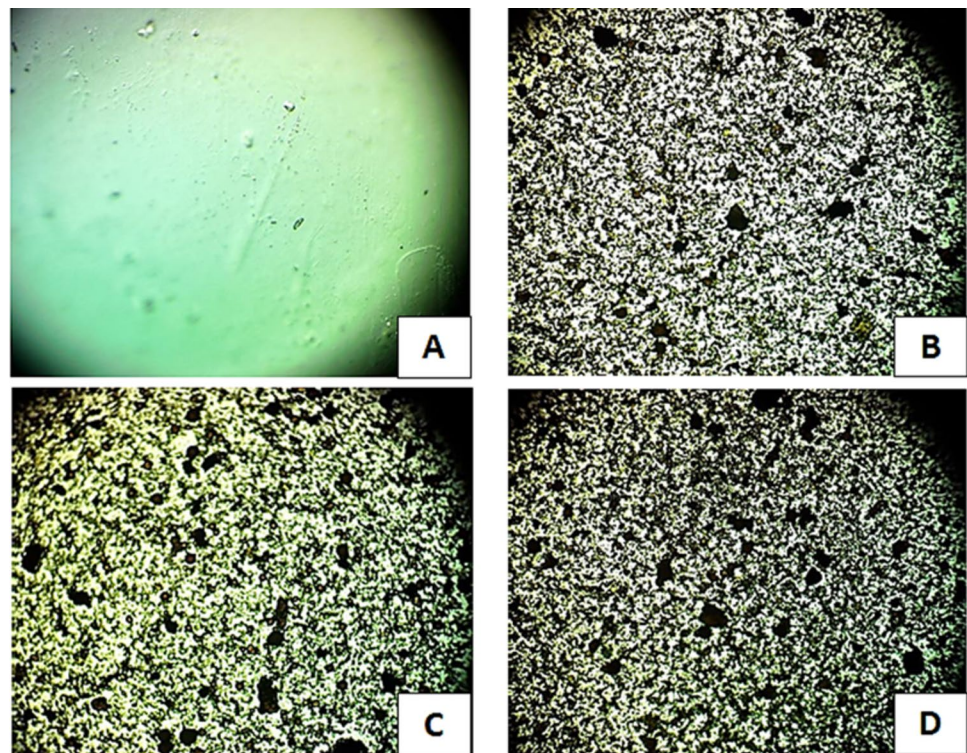
3.1 Optical Microscope of (PVA-SiC-BaTiO₃) NCs

Figure 1 displays images taken with an optical microscope of (PVA-SiC-BaTiO₃) nanocomposites. Different concentrations (2%, 4% and 6%) Wt. were formed as samples. As shown in the images, a magnification of (10x) was used. As a result, the images (A, B, C, and D) differ significantly from one another. When increasing the quantity of (SiC-BaTiO₃) nanoparticles in the PVA matrix, the nanoparticles build an ongoing network inside the polymer, illustrated in 6wt.% for (PVA-SiC-BaTiO₃). This network allows charge carriers to pass through specific channels, which reduces the resistance of the polymeric material (PVA) [14].

3.2 Analysis of (PVA-SiC-BaTiO₃) NCs Using Fourier Transform Infrared rays (FTIR)

Figure 2 displays the (FTIR) transmittance spectra of (PVA-SiC-BaTiO₃) NCs films with different ratios of (SiC-BaTiO₃) nanoparticles obtained in the range ($500\text{--}4000\text{ cm}^{-1}$) at room temperature. Based on this graph shows that the broad bands at 3247 cm^{-1} are caused by (OH) groups. Around 2906 cm^{-1} is the frequency of the band that corresponds to the (CH₂) unbalanced stretching vibration. The C = C stretching mode is supposed to be responsible

Fig. 1 Images of optical microscope to (PVA- SiC- BaTiO₃) NCs at a magnification(10x): **A** PVApure, **B** 2wt.% (SiC-BaTiO₃) NPs, **C** 4wt.% (SiC- BaTiO₃) NPs, **D** 6wt.% (SiC- BaTiO₃) NPs



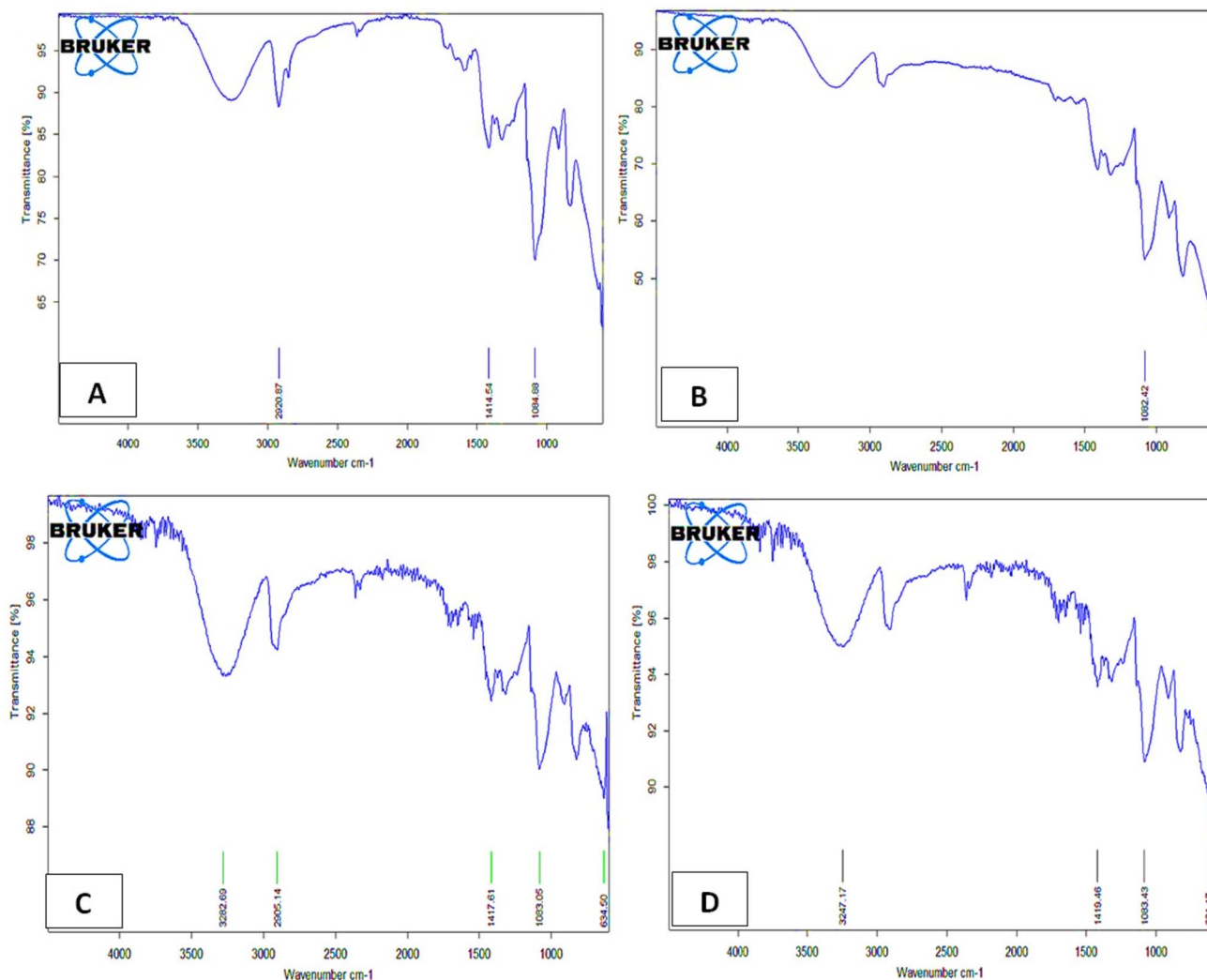


Fig. 2 FTIR spectra for (PVA-SiC-BaTiO₃): **A** (PVA) pure, **B** (2 Wt.%) of (SiC-BaTiO₃) NPs, **C** (4 Wt.%) of (SiC-BaTiO₃) NPs, **D** (6 Wt.%) of (SiC-BaTiO₃) NPs

for the peaks at 1414cm^{-1} . Moreover, the symmetric bending of (CH₂) is what causes the absorbent peak to appear at about 1084cm^{-1} . (PVA) matrix, the (FTIR) spectrum demonstrates a shift in peak location, and also alteration in peak shape and intensity, this indicates that the vibrations of polymer and (SiC-BaTiO₃) nanoparticles are decoupled. The (C – O) band is located around 1082cm^{-1} . In the situation of (PVA- SiC-BaTiO₃) with different (SiC-BaTiO₃) ratios, comparatively to the pure [29].

3.3 The Optical Properties of (PVA- SiC-BaTiO₃) NCs

Figure 3 displays the absorbance for (PVA- SiC-BaTiO₃) nanocomposites films. There is evidence to suggest that silicon carbide-barium titanate filler levels enhance the peak's intensity. Because of the formation of intermolecular

hydrogen bonds between silicon carbide-barium titanate and the nearby groups of the main chain, as well as the movement of the absorption band and the qualitative weight (SiC-BaTiO₃). The (PVA) combination exhibits low absorption because of the wider spacing between the conduction and valence bands. The raised absorbance for (PVA- SiC-BaTiO₃) is caused by an increase in silicon carbide-barium titanate nanoparticles [30, 31].

Figure 4 illustrates the transmittance spectrum of (PVA-SiC-BaTiO₃) NCs with various nanoparticle concentrations vs. incoming light wavelength. The apparent transmittance of (PVA-SiC-BaTiO₃) nanocomposites decreases as the amount of (SiC-BaTiO₃) NPs rises, which is the reverse of the absorbance behavior. This indicates that the (PVA-SiC-BaTiO₃) nanocomposites' absorbance is amended by the (SiC-BaTiO₃) nanoparticles. This is because of the use of (SiC-BaTiO₃) NPs to fill the vacancies between the polymer

Fig. 3 Absorbance of (PVA-SiC-BaTiO₃) NCs depending on wavelength

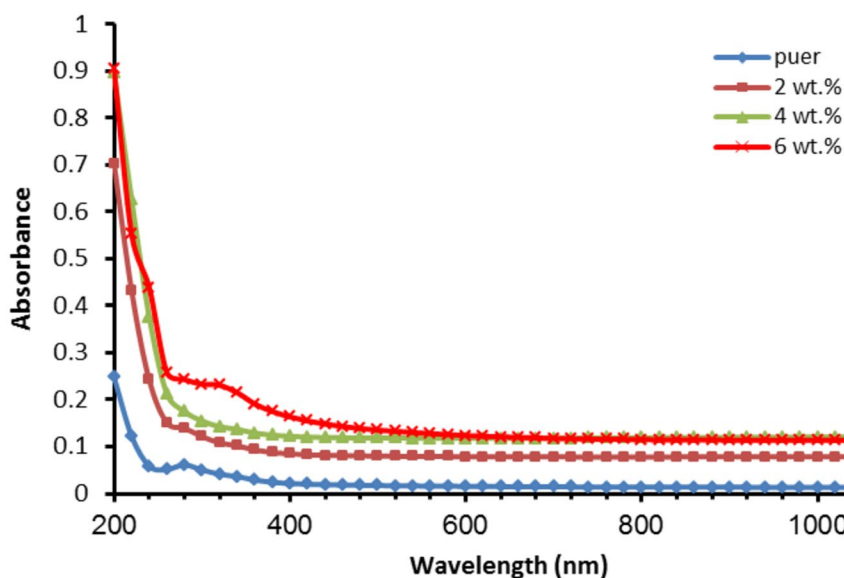
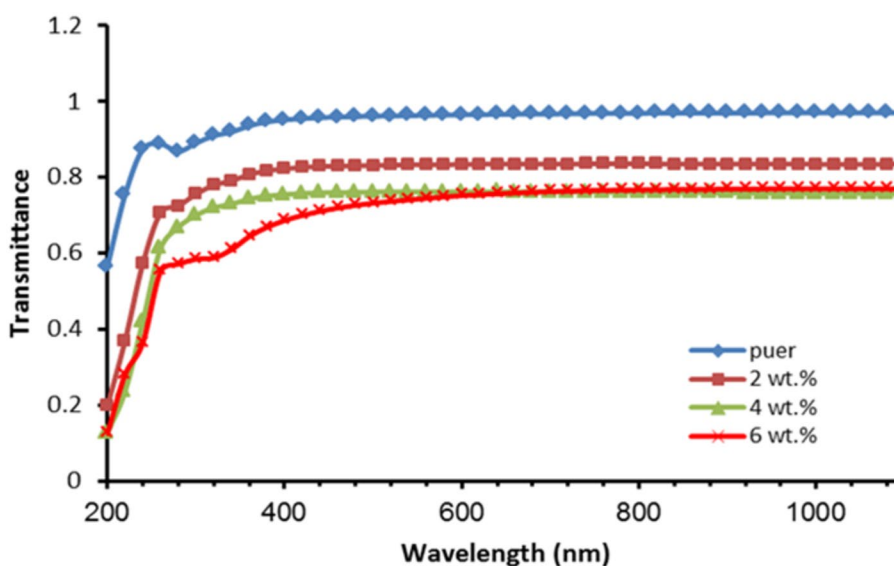


Fig. 4 The transmission spectra of (PVA-SiC-BaTiO₃) NCs as an indicator of wavelength



chains of the moreover, the (SiC-BaTiO₃) nanoparticles' free electrons absorbed the light that impacted the samples, leading them to reach a high energy level and stop emitting any rays. This indicates that the electrons moved to a high level of energy and occupied a vacant space in the energy band. The low transmittance is attributed to the reflection and refraction of light within the samples. It is important to note that the material has a high transmittance. Thus, there are no free electrons in the covalent bonds, which electrons make with the (PVA) atoms. This indicates that several photons are needed to dismantle the covalent bonds and transfer the electrons to the conduction bond [32].

Figure 5 displays the absorption coefficient with photon energy for (PVA-SiC-BaTiO₃). Absorption is impoverished when energy is low. This suggests that there are not many

electron transitions. As photon energy rise, absorption rises as well. This in turn demonstrates the possibility of the transitions of an electron. The absorbance coefficient for (PVA-SiC-BaTiO₃) is enhanced by the addition of (SiC-BaTiO₃) nanoparticles. The advantage of the absorption coefficient in getting the transition electron type. It is projected that there will be more energy direct electron transitions if the absorption coefficient is great. When the absorption coefficient is low, an indirect transition of electrons is anticipated since photons and electrons can both preserve energy and momentum. Only phonons have the ability to conserve momentum. These result is agree with other researchers results [33, 34]. The results show that there is an indirect energy band gap since the absorption coefficient for (PVA-SiC-BaTiO₃) is smaller than 10^4 cm^{-1} .

Fig. 5 The correlation between the photon energy and the absorption coefficient of (PVA-SiC-BaTiO₃) NCs

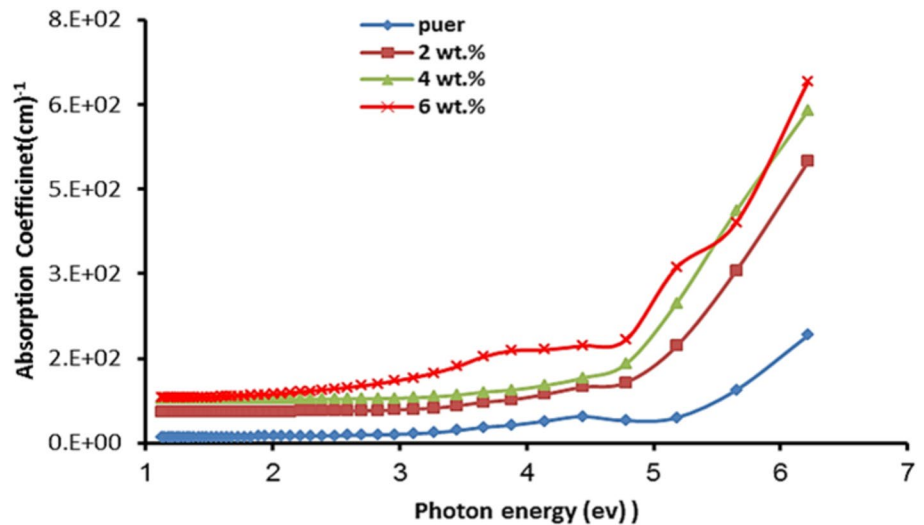


Figure 6 illustrates how the absorbance edge $(\alpha h\nu)^{1/2}$ varies with photon energy for (PVA-SiC-BaTiO₃) NCs. Draw a straight line from the curve's highest point to the axis (X) at the position when $(\alpha h\nu)^{1/2} = 0$ (allowable), we get into an indirect energy gap transition. Table 1 indicates that the values of the indirect energy gap (allowed) of (PVA-SiC-BaTiO₃) nanocomposites decline as the concentration of (SiC-BaTiO₃) rises. This suggests that there are significant localized levels in the confined energy gap. These result is agree with other researchers results [35, 36].

The changes in the absorbance edge $(\alpha h\nu)^{1/3}$ for (PVA-SiC-BaTiO₃) as a function of 'photon energy' are displayed in Fig. 7. It demonstrates that: the indirect energy gap (prohibit) for (PVA-SiC-BaTiO₃) reduces as the concentration of (SiC-BaTiO₃) NPs rises, as seen in Table 1,

demonstrating that this feature aids in the creation of new levels. Additionally, transitions of electrons between novel levels tails produced by the additive (SiC-BaTiO₃). These result is agree with researcher results [37].

Figure 8 illustrates the extinction coefficient (k) of (PVA-SiC-BaTiO₃) changes with wavelength, through increasing the quantity of (SiC-BaTiO₃) nanoparticles in the (PVA) polymer, increasing(k). The extinction coefficient behavior suggests significant absorption. Additionally, polarization of the medium charges is caused by the interaction of the carrying charge in the samples with the incident light, Thus, causes the energy of the incident photon to be lost. This indicates that the (SiC-BaTiO₃) nanoparticles modify the host (PVA) polymer. It is an interesting finding that the absorption rises in the visible range as the amount of (SiC-BaTiO₃) nanoparticles increases [38].

Fig. 6 Illustrates the variation of $(\alpha h\nu)^{1/2}$ for (PVA-SiC-BaTiO₃) with photon energy

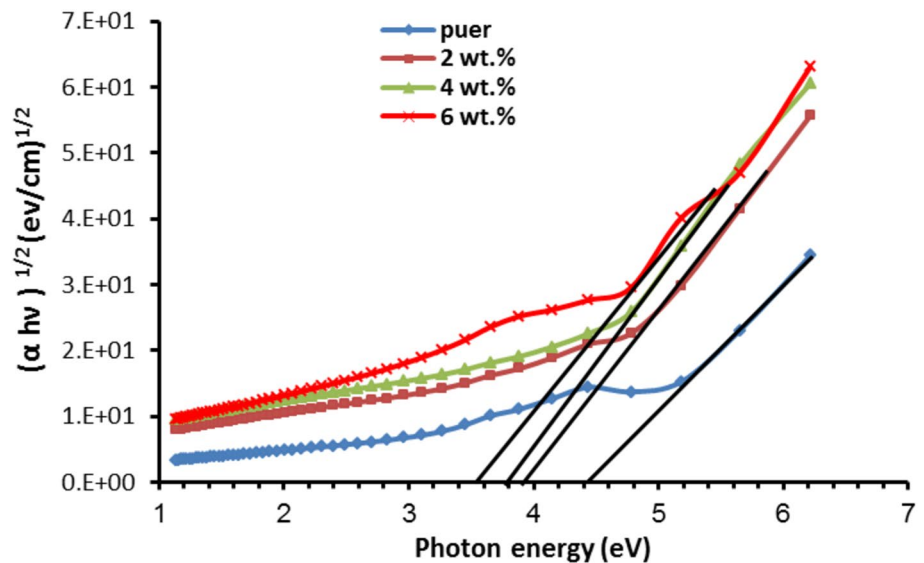


Fig. 7 Illustrates the variation of $(\alpha h\nu)^{1/3}$ for (PVA- SiC-BaTiO₃) with photon energy

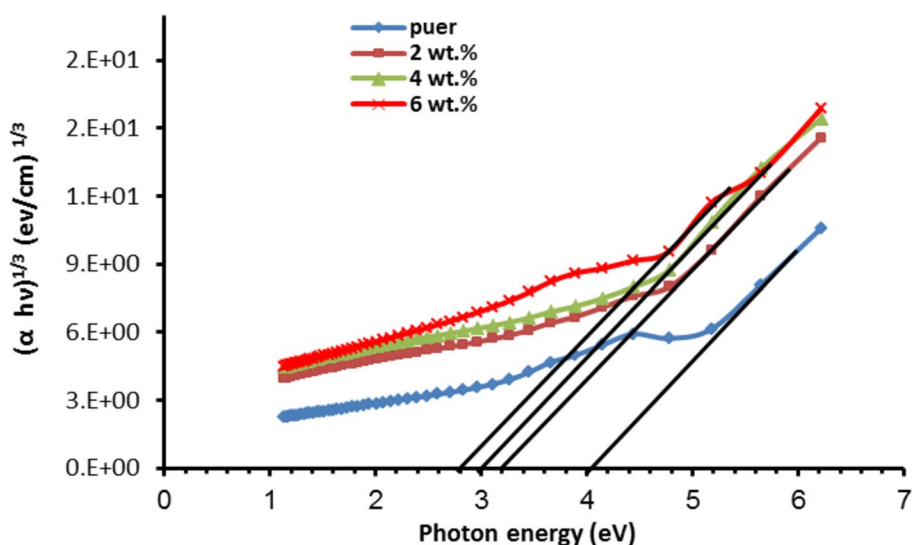


Table 1 Displays the energy gaps for the indirect transition for (PVA-SiC-BaTiO₃) NCs (both allowed and forbidden)

Con. of (SiC-BaTiO ₃) NCs wt%	Indirect energy gap (allowed) eV	Indirect energy gap (forbidden) eV
0	4.42	4.1
2	3.93	3.24
4	3.81	3.1
6	3.56	2.85

Figure 9 demonstrates how the refractive index (n) of (PVA-SiC-BaTiO₃) nanocomposites varies with wavelength. With increased incoming photon scattering, the refractive index of the (PVA) polymer raises with increasing (SiC-BaTiO₃) nanoparticle concentration, so the reflection increases. Moreover, the (PVA -SiC-BaTiO₃)

nanocomposites’ intensity improves with the addition of additional (SiC-BaTiO₃) nanoparticles. Strong reflection occurs when incident light hits a (PVA) polymer that contains (SiC-BaTiO₃) nanoparticles. This results in an amended reflectivity for (PVA-SiC-BaTiO₃) [39].

Figures 10 and 11 display the variations regarding (PVA-SiC-BaTiO₃) nanocomposites. The “real and imaginary” parts of the dielectric constant (ϵ_1, ϵ_2) are shown against wavelength, respectively. As for the actual dielectric constant in Fig. 10 increases with the rises in the concentration (SiC-BaTiO₃) of nanoparticles because of the increase in conductivity and density of charge carriers. It can be said that the real component is bigger than the imaginary component since it is primarily proportional to the square of the (n). According to Fig. 11, the imaginary portion is proportional to the extinction coefficient, and

Fig. 8 The wavelength effect on the extinction coefficient for (PVA- SiC- BaTiO₃) NCs

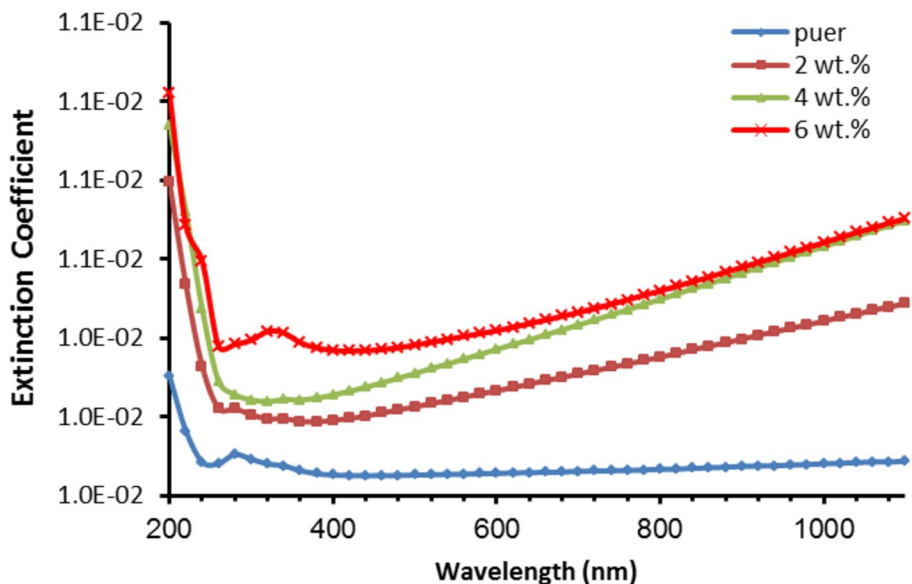


Fig. 9 Refractive index for (PVA-SiC-BaTiO₃) as a function of wavelength

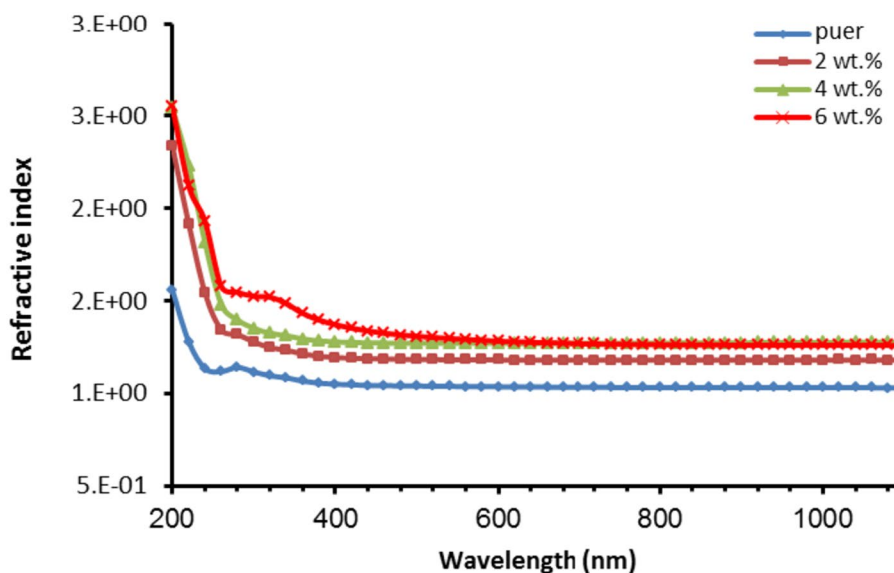
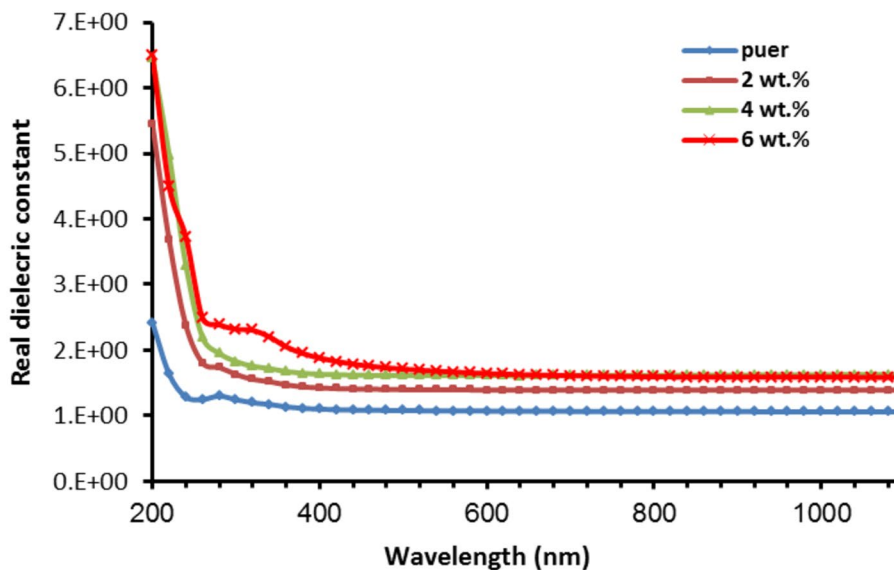


Fig. 10 Real dielectric constant for (PVA-SiC-BaTiO₃) NCs as a function of wavelength



it rises with an increase in (SiC-BaTiO₃), while the real component rises with an increase in the additive (SiC-BaTiO₃). These results are agree with other researchers results [40, 41].

Figure 12 illustrates the optical conductivity for (PVA-SiC-BaTiO₃) nanostructures as a function of wavelength. The (PVA) polymer behaves differently from the (PVA-SiC-BaTiO₃) nanocomposites. At raising photon energies, optical conductivity increases, while at lower photon energies, it decreases. Furthermore, the optical conductivity of (PVA-SiC-BaTiO₃) nanocomposites is improved by the inclusion of (SiC-BaTiO₃) nanoparticles [42].

3.4 The A.C Electrical Features of (PVA-SiC-BaTiO₃) NCs

Figure 13 displays the (PVA-SiC-BaTiO₃) nanocomposites frequency-dependent dielectric constant variation. This graphic illustrates how the dielectric constant varies as frequency gets higher. This behavior is described by a decrease in the polarization of space charges compared to total polarization. An ion mass is greater than that of an electron, and an ion reacts to changes in field frequencies more slowly than electronic polarization does. The electrons interact even at high field vibration frequencies. The dielectric constant is

Fig. 11 The imaginary component of the dielectric constant for (PVA-SiC-BaTiO₃) NCs as a function of wavelength

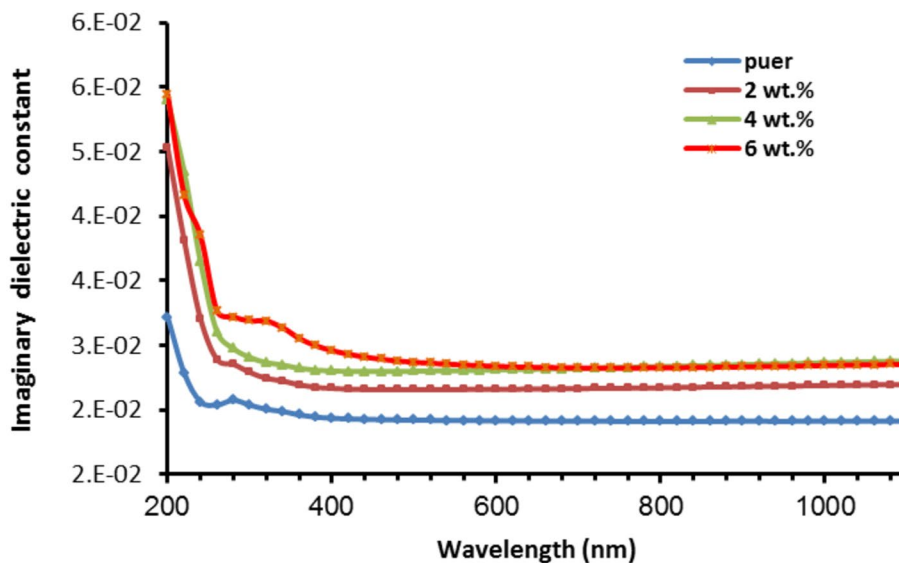
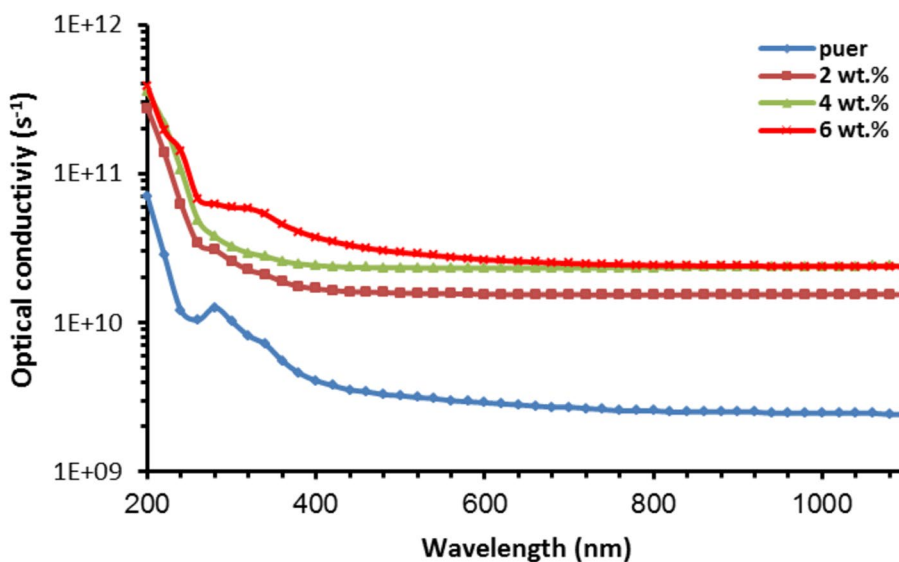


Fig. 12 The variation in optical conductivity of (PVA-SiC-BaTiO₃) with wavelength



virtually identical across all samples when tested at extreme frequencies since there aren't any novel kinds of polarization at higher frequencies due to the low electron mass [43, 44]. Figure 14 illustrates how the dielectric constant increase as the weight ratios of nanoparticles increase. The dielectric constant increases with increasing of the concentrations of (SiC-BaTiO₃) nanoparticles. This behavior may be a return to interfacial polarization inside the nanocomposites in applied electric field and an increase in charge carriers when polarization occurs and thus an increase in the value of the dielectric constant. These results are agree with researcher results [45].

Figure 15 displays the frequency-dependent dielectric loss of (PVA-SiC-BaTiO₃) nanocomposites. According to this graph, a decrease in dielectric loss results from an

increase in frequency. This is due to mobile charges that are present inside the polymer backbone. This happens because there are more electrons in nanocomposites, which decreases the contribution of space charge polarization as frequency increases [46]. Moreover, at intermediate frequencies, the (ϵ'') of (PVA-SiC-BaTiO₃) nanocomposites is significant and decreases with rising frequency. As can be observed in Fig. 16, the ϵ'' grows as the concentration of (SiC-BaTiO₃) nanoparticles in the nanocomposite increases. The increases in the concentration of SiC-BaTiO₃ nanoparticles lead to an increase in the number of ionic charge carriers, which in turn leads to a rise in the value of the dielectric loss. This phenomenon can be observed when the weight% content of nanoparticles increases. These results are agree with other researchers results [47, 48].

Fig. 13 The ϵ' for (PVA-SiC-BaTiO₃)NCs as a function of frequency

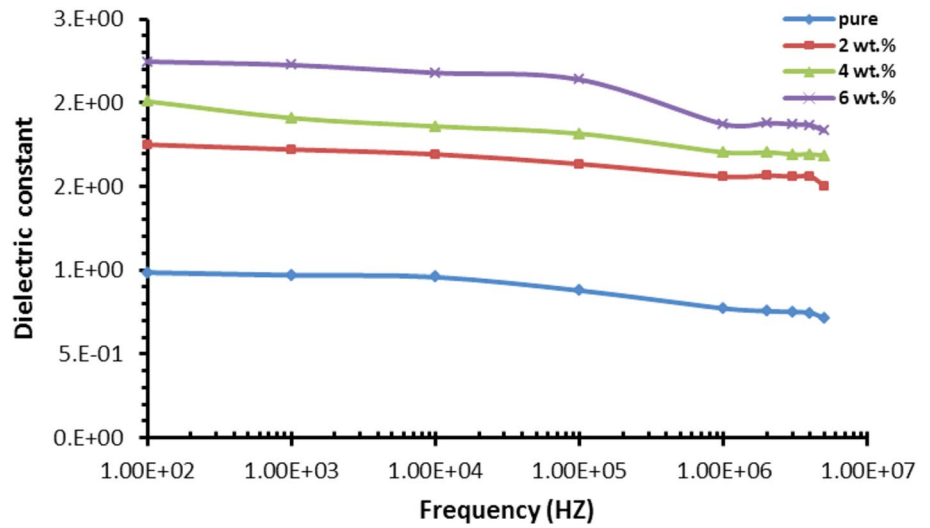


Fig. 14 Influence of (SiC-BaTiO₃) content on the ϵ' of (PVA-SiC-BaTiO₃) at 100 Hz

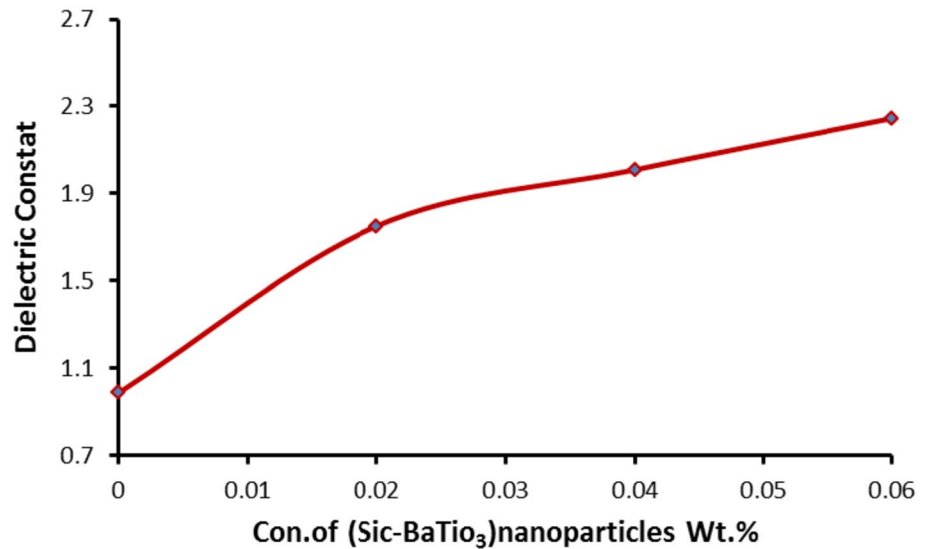


Fig. 15 The ϵ'' for (PVA-SiC-BaTiO₃) nanocomposites with varying frequency

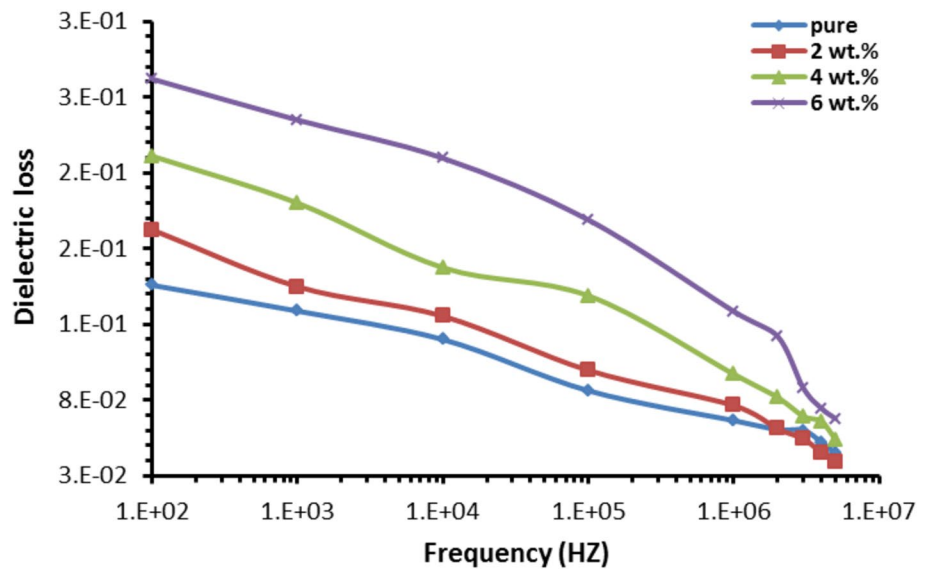


Fig. 16 Influence of (SiC-BaTiO₃) content on the ϵ'' of (PVA-SiC-BaTiO₃) at 100 Hz

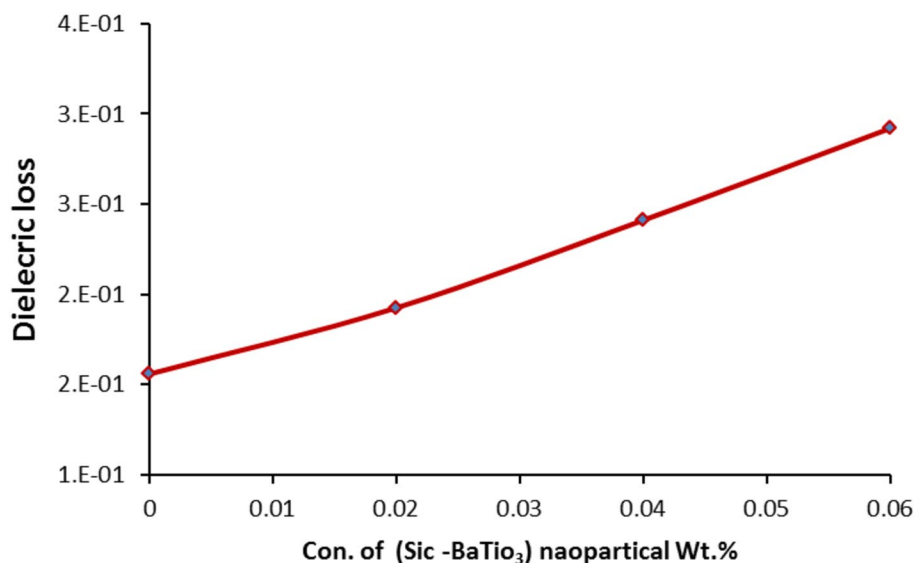


Fig. 17 The A.C conductivity for (PVA-SiC-BaTiO₃) NCs varies with frequency

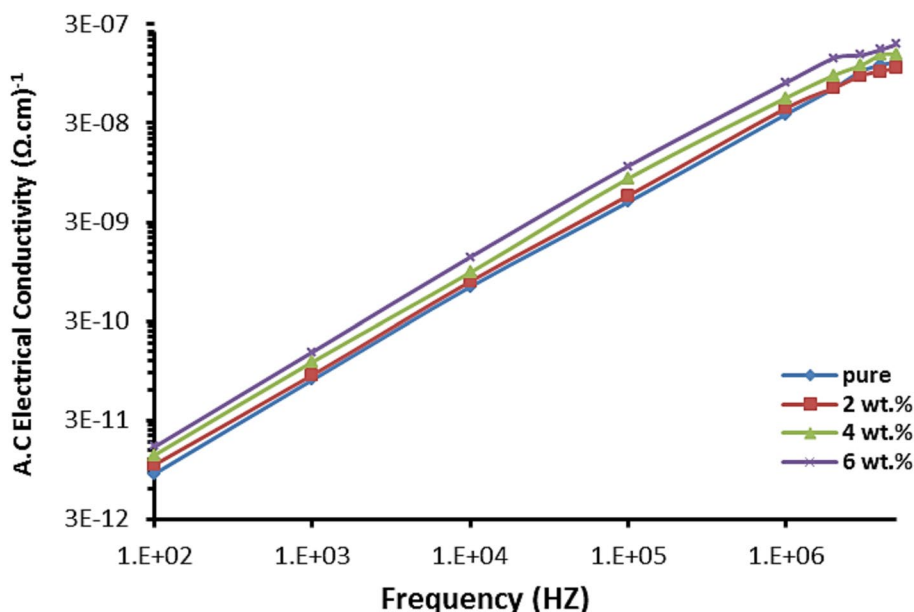


Figure 17 shows A.C. electrical conductivity varies with frequency for (PVA-SiC-BaTiO₃) NCs. From this figure, when the electric field rises, all samples A.C conductivity significantly rises; this is due to space charge polarization, which happens at lower frequencies, further to charge carrier jumping motion. Since there are greater charge carriers brought on by their regular distribution throughout the (PVA), the observed change may be attributed to the effect of the space charge [49].

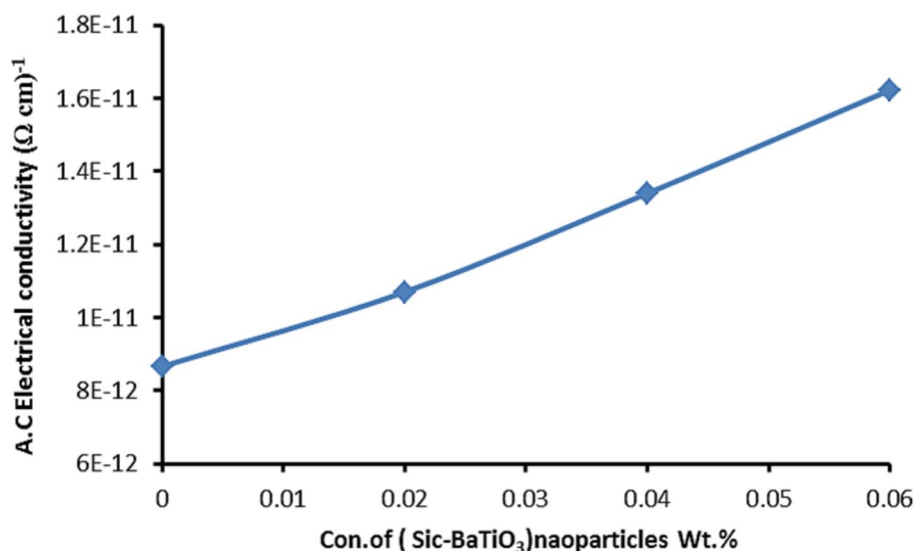
Figure 18 illustrates that when the weight% of (SiC-BaTiO₃) NPs gets larger, the conductivity rises. The observed increase in conductivity can be attributed to the increase in the number of charge carriers resulting from the presence of dopant nanoparticles in the composition of the

nanocomposites. This, in turn, leads to a gradual reduction in resistance and a subsequent rise in A.C electrical conductivity. Moreover, the SiC-BaTiO₃ nanoparticles establish a continuous network of pathways within the polymer matrix that facilitate the conduction of charge carriers, particularly when the nanoparticles concentration is at 6 wt%, in the case of (PVA-SiC-BaTiO₃) nanocomposites [50].

4 Conclusion

In this work, (PVA-SiC-BaTiO₃) polymer films were prepared utilizing the solution casting method. The distribution of the (SiC-BaTiO₃) additions was homogenous, according

Fig. 18 Variation of electrical conductivity for (PVA-SiC-BaTiO₃) NCs with (SiC-BaTiO₃) NPs content



to optical microscope images, and the nanoparticles formed a continuous network inside the polymer mixture. (FTIR) investigate revealed that (PVA-SiC-BaTiO₃) allow for just a small amount vibrational molecular mobility. As the concentration of (SiC-BaTiO₃) NPs rises, the absorbance, absorption coefficient, refractive index, extinction coefficient, (real and imaginary) dielectric constant, and optical conductivity all rise for (PVA-SiC-BaTiO₃) NCs. The energy gap for permitted and prohibited indirect transitions decreased from (4.42 to 3.56) eV and from (4.1 to 2.85) eV, respectively. Transmittance decrease with increasing of (SiC-BaTiO₃) ratios. Because of its characteristics, (PVA-SiC-BaTiO₃) nanocomposites can be regarded as a good optical material for photonics applications. The (PVA-SiC-BaTiO₃) nanocomposites dielectric properties revealed that the dielectric constant, dielectric loss, and (σ_{ac}) are rise from (0.98 to 2.24), (0.15 to 0.29) and (8.6×10^{-12} to 1.6×10^{-11}) ($\Omega \cdot \text{cm}$)⁻¹ respectively (at $f = 100$ Hz), as (SiC-BaTiO₃) nanoparticles increase. As frequency rises, alternating current's (A.C.) electrical conductivity rises while the dielectric constant and dielectric loss drop. The (PVA-SiC-BaTiO₃) nanostructures' optical and dielectric properties imply that they might be employed in a variety of flexible nanoelectronic applications with high energy storage, little loss, lightweight and low cost.

Author Contributions All authors contributed to the study conception and design. Material preparation, data collection and analysis were performed by MAH and WKK. The first draft of the manuscript was written by Majeed Ali Habeeb and all authors commented on previous versions of the manuscript. All authors read and approved the final manuscript.

Funding The authors have not disclosed any funding.

Data Availability Available.

Declarations

Conflict of interest No conflict of interest.

Ethics Approval The Research is not involving the studies on human or their data.

Consent to Participate Consent.

Consent for Publication Consent.

References

1. T.P. Nguyen, Polymer-based nanocomposites for organic optoelectronic devices. A review. *Surf. Coat. Technol.* **206**(4), 742–752 (2011). <https://doi.org/10.1016/j.surfcoat.2011.07.010>
2. A.H. Hadi, M.A. Habeeb, The dielectric properties of (PVA-PVP-CdS) nanocomposites for gamma shielding applications. *J Phys.: Conf. Ser.* **1973**(1), 01206310 (2021).
3. S.M. Mahdi, M.A. Habeeb, Low-cost piezoelectric sensors and gamma ray attenuation fabricated from novel polymeric nanocomposites. *AIMS Mater. Sci.* **10**(2), 288–300 (2023). <https://doi.org/10.3934/matserci.2023015>
4. S. Mallakpour, H.Y. Nazari, The influence of bovine serum albumin-modified silica on the physicochemical properties of poly(vinyl alcohol) nanocomposites synthesized by ultrasonication technique. *Ultrason. Sonochem.* **41**, 1–10 (2018). <https://doi.org/10.1016/j.ultsonch.2017.09.017>
5. O.G. Abdullah, S.B. Aziz, K.M. Omer, Y.M. Salih, Reducing the optical band gap of polyvinyl alcohol (PVA) based nanocomposite. *J. Mater. Sci.: Mater. Electron.* **26**, 5303–5309 (2015). <https://doi.org/10.1007/s10854-015-3067-3>
6. N. Hayder, M.A. Habeeb, A. Hashim, Structural, optical and dielectric properties of (PS-In₂O₃/ZnCoFe₂O₄) nanocomposites. *Egypt. J. Chem.* **63**, 577–592 (2020). <https://doi.org/10.21608/ejchem.2019.14646.1887>
7. Q.M. Jebur, A. Hashim, M.A. Habeeb, Structural, A.C electrical and optical properties of (polyvinyl alcohol-polyethylene oxide-aluminum oxide) nanocomposites for piezoelectric devices. *Egypt. J. Chem.* **63**, 719–734 (2020). <https://doi.org/10.21608/ejchem.2019.14847.1900>

8. M.B. Mohamed, M.H. Abdel-Kader, Effect of excess oxygen content within different nano-oxide additives on the structural and optical properties of PVA/PEG blend. *Appl. Phys. A* **125**(3), 1–11 (2019)
9. M.A. Habeeb, A. Hashim, N. Hayder, Fabrication of (PS-Cr₂O₃/ZnCoFe₂O₄) nanocomposites and studying their dielectric and fluorescence properties for IR sensors. *Egypt. J. Chem.* **63**, 709–717 (2020). <https://doi.org/10.21608/ejchem.2019.13333.1832>
10. Z. Ping, Q.T. Nguyen, A.Essamri, and, J.N. el, Polym. Adv. Technol. " *Macromol. Chem. Phys. No.* **195**, 21–31 (1994)
11. K. Sreekanth, T. Siddaiah, N.O. Gopal, Y. Madhava Kumar, Ramu Optical and electrical conductivity studies of VO²⁺ doped polyvinyl pyrrolidone (PVP) polymer electrolytes. *J. Science: Adv. Mater. Devices* ISBN **4**, 230–236 (2019)
12. M.A. Habeeb, W.S. Mahdi, Characterization of (CMC-PVP-Fe₂O₃) nanocomposites for gamma shielding application. *Int. J. Emerg. Trends Eng. Res.* **7**(9), 247–255 (2019). <https://doi.org/10.30534/ijeter/2019/06792019>
13. L.H. Gaabour, Influence of silica nanoparticles incorporated with chitosan/polyacrylamide polymer nanocomposites. *J. Mater. Res. Technol.* **8**(2), 2157–2163 (2019)
14. M.A. Habeeb, A. Hashim, N. Hayder, Structural and optical properties of novel (PS-Cr₂O₃/ZnCoFe₂O₄) nanocomposites for UV and microwave shielding. *Egypt. J. Chem.* **63**, 697–708 (2020). <https://doi.org/10.21608/ejchem.2019.12439.1774>
15. M.A. Habeeb, Effect of rate of deposition on the optical parameters of GaAs films. *Eur. J. Sci. Res.* **57**(3), 478–484 (2011)
16. M.A. Habeeb, Dielectric and optical properties of (PVAc-PEG-Ber) biocomposites. *J. Eng. Appl. Sci.* **9**(4), 102–108 (2014). <https://doi.org/10.36478/jeasci.2014.102.108>
17. T. Soliman, S. Vshivkov, Effect of Fe nanoparticles on the structure and optical properties of polyvinyl alcohol nanocomposite films. *J. Non-cryst. Solids.* **519**, 119452 (2019)
18. M.S. Micozzi, F.M. Townsend, C.E. Koop, From Army Medical Museum to national museum of health and medicine. A century-old institution on the move. *Arch. Pathol. Lab. Med.* **114**(12), 1290–1295 (1990)
19. S.M. Mahdi, M.A. Habeeb, Synthesis and augmented optical characteristics of PEO–PVA–SrTiO₃–NiO hybrid nanocomposites for optoelectronics and antibacterial applications. *Opt. Quant. Electron.* **54**, 854 (2022). <https://doi.org/10.1007/s11082-022-04267-6>
20. J. Tauc, A. Menth, D.L. Wood, Optical and magnetic investigations of the localized states in semiconducting glasses. *Phys. Rev. Lett.* **25**(11), 749–758 (1970)
21. A. Alshehari, E. Salim, A. Oraby, Structural, optical, morphological and mechanical studies of polyethylene oxide/sodium alginate blend containing multi-walled carbon nanotubes. *J. Mater. Res. Technol.* **15**, 5615–5622 (2021)
22. S.S. Manhas, P. Rehan, A. Kaur, A.D. Acharya, B. Sarwan, Evaluation of optical properties of polypyrrole: Polystyrene nanocomposites. *AIP Conf. Proc.* **2100**(4), 1–5 (2019). <https://doi.org/10.1063/1.5098591>
23. K.L. Chopra, P.D. Paulson, V. Dutta, Thin film solar cells: an overview. *Prog. Photovolt. Res. Appl.* **12**(2), 69–92 (2004)
24. M.A. Habeeb, Z.S. Jaber, W.H. Radi, Synthesis and characterization of (PVA-CoO-ZrO₂) nanostructures for Nanooptoelectronic Fields. *East Eur. J. Phys.* **2**, 228–233 (2023). <https://doi.org/10.26565/2312-4334-2023-2-25>
25. S. Kramadhathi, K. Thyagarajan, Optical properties of pure and doped (KnO₃ & MgCl₂) polyvinyl alcohol polymer thin films. *Int. J. Thin Film Sci. Technol.* **6**(8), 15–18 (2013)
26. N.K. Al-Sharifi, M.A. Habeeb, Improvement structural and dielectric properties of PS/SiC/Sb₂O₃ nanostructures for nanoelectronics devices. *East Eur. J. Phys.* **2**, 341–347 (2023). <https://doi.org/10.26565/2312-4334-2023-2-40>
27. S.M. Mahdi, M.A. Habeeb, Fabrication and tailored structural and dielectric characteristics of (SrTiO₃/ NiO) nanostructure Doped (PEO/PVA) polymeric blend for Electronics Fields. *Phys. Chem. Solid State.* **23**(4), 785–792 (2022). <https://doi.org/10.15330/pcss.23.4.785-792>
28. Y. Wang, S. Dong, X. Li, C. Hong, X. Zhang, Synthesis, properties, and multifarious applications of SiC nanoparticles. *Rev. Ceram. Int.* **48**(7), 8882–8913 (2022)
29. A. Hashim, M.A. Habeeb, Q.M. Jebur, Structural, dielectric and optical properties for (polyvinyl alcohol-polyethylene oxide manganese oxide) nanocomposites. *Egypt. J. Chem.* **63**, 735–749 (2020). <https://doi.org/10.21608/ejchem.2019.14849.1901>
30. M.A. Habeeb, W.K. Kadhim, Study the optical properties of (PVA-PVAc-Ti) nanocomposites. *J. Eng. Appl. Sci.* **9**(4), 109–113 (2014). <https://doi.org/10.36478/jeasci.2014.109.113>
31. M.A. Habeeb, Z.S. Jaber, Enhancement of structural and optical properties of CMC/PAA blend by addition of zirconium carbide nanoparticles for optics and photonics applications. *East Eur. J. Phys.* **4**, 176–182 (2022). <https://doi.org/10.26565/2312-4334-2022-4-18>
32. A.H. Hadi, M.A. Habeeb, Effect of CdS nanoparticles on the optical properties of (PVA-PVP) blends. *J. Mech. Eng. Res. Dev.* **44**(3), 265–274 (2021)
33. A. Shubha, S.R. Manohara, L. Gerward, Influence of polyvinyl pyrrolidone on optical, electrical, and dielectric properties of poly (2-ethyl-2-oxazoline)-polyvinyl pyrrolidone blends. *J. Mol. Liq.* **247**, 328–336 (2017)
34. S.M. Mahdi, M.A. Habeeb, Tailoring the structural and optical features of (PEO–PVA)/(SrTiO₃–CoO) polymeric nanocomposites for optical and biological applications. *Polym. Bull.* (2023). <https://doi.org/10.1007/s00289-023-04676-x>
35. K.M.K. Sudha, K.H.G. Harish, R. Chandramani, M.C. Radhakrishna, PVP influence on PVA crystallinity and optical band gap. *Arch. Phy Res.* **6**, 18–21 (2015)
36. M.H. Dwech, M.A. Habeeb, A.H. Mohammed, Fabrication and evaluation of optical characteristics of (PVA-MnO₂–ZrO₂) nanocomposites for Nanodevices in Optics and Photonics. *Ukr. J. Phys.* **67**(10), 757–762 (2022). <https://doi.org/10.15407/ujpe67.10.757>
37. S.H. Yu, M. Yoshimura, J.M.C. Moreno, T. Fujiwara, T. Fujino, R. Teranishi, In situ fabrication and optical properties of a novel polystyrene/semiconductor nanocomposite embedded with CdS nanowires by a soft solution processing route. *Langmuir.* **17**(5), 1700–1707 (2001). <https://doi.org/10.1021/la000941p>
38. N.K. Al-Sharifi, M.A. Habeeb, Synthesis and exploring structural and optical properties of Ternary PS/SiC/Sb₂O₃ nanocomposites for optoelectronic and antimicrobial applications. *Silicon.* **15**, 4979–4989 (2023)
39. A.A. Mohammed, M.A. Habeeb, Modification and development of the structural, optical and antibacterial characteristics of PMMA/ Si₃N₄/TaC nanostructures. *Silicon* **15**, 5163–5174 (2023). <https://doi.org/10.1007/s12633-023-02426-2>
40. R.S. Abdul Hamza, M.A. Habeeb, Synthesis and tuning the structural, morphological and dielectric characteristics of PVA-CMC-SiO₂-Cr₂O₃ hybrid nanostructures for nanoelectronics devices. *Opt. Quant. Electron.* **55**(8), 705 (2023)
41. K. Rajesh, V. Crasta, N. Rithin Kumar, G. Shetty, P. Rekha, Structural, optical, mechanical and dielectric properties of titanium dioxide doped PVA/PVP nanocomposite. *J. Polym. Res.* **26**(4), 1–10 (2019)
42. U. Kumar, D. Padalia, L. Lendvai, P. Bhandari, P.K.L. Ranakoti, Fabrication of europium-doped barium titanate/polystyrene polymer nanocomposites using ultrasonication-assisted method: Structural and optical properties. *Polym (Basel).* **14**(21), 4664 (2022). <https://doi.org/10.3390/polym14214664>
43. M.A. Habeeb, R.S. Abdul Hamza, Novel of (biopolymer blend-MgO) nanocomposites: fabrication and characterization for

- humidity sensors. *J. Bionanosci.* **12**, 328–335 (2018). <https://doi.org/10.1166/jbns.2018.1535>
44. M.A. Habeeb, R.S.A. Hamza, Synthesis of (polymer blend–MgO) nanocomposites and studying electrical properties for piezoelectric application. *Indonesian J. Electr. Eng. Inf.* **6**(4), 428–435 (2018). <https://doi.org/10.11591/ijeel.v6i1.511>
 45. G.D. Liang, S.C. Tjong, Electrical properties of percolative polystyrene/carbon nanofiber composites. *IEEE Trans. Dielectr. Electr. Insul.* **15**(1), 214–220 (2008)
 46. S.M. Mahdi, M. A. Habeeb, Evaluation of the influence of SrTiO₃ and CoO nanofillers on the structural and electrical polymer blend characteristics for electronic devices. *Digest J. Nanomater. Biostr.* **17**(3), 941–948 (2022). <https://doi.org/10.15251/DJNB.2022.173.941>
 47. M.A. Habeeb, A.H. Mohammed, Fabrication and tailored optical and electrical characteristics of Co₂O₃/SiC nanostructures doped PVA for multifunctional technological applications. *Opt. Quant. Electron.* **55**, 791 (2023). <https://doi.org/10.1007/s11082-023-05061-8>
 48. K.M. Vidyalaya, Analysis of electrical properties of Li³⁺ ion beam irradiated lexan polycarbonate also act as catalyst to speed up the discoloration. *The Formation of Conjugated* **21**(10), 43–46 (2009)
 49. M.A. Habeeb, W.H. Rahdi, Titanium carbide nanoparticles filled PVA–PAAm nanocomposites, structural and electrical characteristics for application in energy storage. *Opt. Quant. Electron.* **55**, 334 (2023). <https://doi.org/10.1007/s11082-023-04639-6>
 50. A.A. Mohammed, M.A. Habeeb, Effect of Si₃N₄/TaC nanomaterials on the structural and electrical characteristics of poly methyl methacrylate for electrical and electronics applications. *East Eur. J. Phys.* **2**, 157–164 (2023). <https://doi.org/10.26565/2312-4334-2023-2-15>

Publisher's Note Springer Nature remains neutral with regard to jurisdictional claims in published maps and institutional affiliations.

Springer Nature or its licensor (e.g. a society or other partner) holds exclusive rights to this article under a publishing agreement with the author(s) or other rightsholder(s); author self-archiving of the accepted manuscript version of this article is solely governed by the terms of such publishing agreement and applicable law.